Climate specific accelerated ageing tests & evaluation of ageing induced electrical, physical and chemical changes

Article *in* Progress in Photovoltaics Research and Applications · November 2018

DOI: 10.1002/pip.3090

CITATION
1

READS
206

9 authors, including:

Gabriele Eder
OFI Österreichisches Forschungsinstitut für Chemie und Technik
91 PUBLICATIONS **1,658** CITATIONS
SEE PROFILE

Yuliya Voronko
Österreichisches Forschungsinstitut (OFI)
24 PUBLICATIONS **75** CITATIONS
SEE PROFILE

Karl Knöbl
University of Applied Science, Technikum Wien
10 PUBLICATIONS **16** CITATIONS
SEE PROFILE

Karl Anton Berger
AIT Austrian Institute of Technology
36 PUBLICATIONS **193** CITATIONS
SEE PROFILE

Received: 7 July 2018 | Revised: 2 October 2018 | Accepted: 15 October 2018

DOI: 10.1002/pip.3090

EU PVSEC PAPER

WILEY PROGRESS IN PHOTOVOLTAICS

Climate specific accelerated ageing tests and evaluation of ageing induced electrical, physical, and chemical changes

Gabriele C. Eder[1] | Yuliya Voronko[1] | Simon Dimitriadis[2] | Karl Knöbl[2] | Gusztáv Újvári[3] | Karl A. Berger[3] | Martin Halwachs[3] | Lukas Neumaier[4] | Christina Hirschl[4]

[1] OFI, Austrian Research Institute for Chemistry and Technology, Franz Grill Str. 1, 1030 Wien, Austria

[2] FH-TW, University of Applied Sciences, Vienna, Austria

[3] AIT, Austrian Institute of Technology, Austria

[4] CTR, Carinthian Tech Research AG, Austria

Correspondence
Gabriele Eder, OFI, Austrian Research Institute for Chemistry and Technology, Franz Grill Str. 1, 1030 Wien, Austria.
Email: gabriele.eder@ofi.at

Funding information
Austrian Climate and Energy Fund; Austrian Research Promotion Agency; Austrian Climate and Energy Fund

Abstract

As the PV market shows enormous potential with huge growth rates especially in climatic-sensible regions, specific artificial ageing test procedures are a key point for an efficient and fast product development of new PV modules/materials optimized for the use in specific climatic regions. Based on the definition of four climate profiles (dry and hot—arid, moderate, humid, and hot—tropical and high irradiation—alpine), a program was worked out with 14 climate specific test conditions for accelerated ageing tests. The big challenge in this respect was the adaption/advancement of existing standard procedures for PV modules/components testing in a way that reliable testing for certain climatic conditions optimized PV modules is possible. The time-dependent repeated application of combined climatic and environmental stresses (temperature, temperature cycles, humidity, irradiation, mechanical load, salt mist) was used to induce performance losses, material degradation, and failures in test modules which resemble those effects occurring in real-life PV installations under comparable climatic and environmental conditions. For this demanding task, a large number of identical test modules with respect to composition and module design was manufactured. A detailed nondestructive analysis/characterization of all modules was performed: (1) before; (2) during (six intermediate stages); and (3) after the accelerated ageing test. The nondestructive characterization methods used to follow the module's ageing processes throughout the whole accelerated ageing procedure were current-voltage characteristics measurements and electroluminiscence images for the electrical performance evaluation and ultraviolet fluorescence (spectroscopic and imaging) measurements, Fourier transform infrared spectroscopy as well as colour measurements of the backsheets outer layer for recording of chemical changes of the encapsulant and backsheet. The electrical and material characterization data were incorporated in an optimized database. As stated above, a set of three identical modules was exposed together in the respective climate specific ageing tests and subsequently characterized in order to increase statistical reliability of the measuring results. The analysis of the data and first approaches of advanced data treatment have already clearly shown that the electrical and material degradation of the test modules is dependent on (1) the type and combination, (2) duration, and (3) mode (sequential versus constant) of the stresses applied. On

the one hand, the simulation of environmental stresses like heavy snow and wind load and enhanced frequency of temperature cycling resulting in cell cracks and cell connector breakage could be demonstrated. Additional treatment in salty atmosphere, on the other hand, did not show an accelerating effect on degradation on the electrical or material side. The accelerating effect of enhanced temperature, humidity, or additional irradiation on the degradation of power and materials could be shown very well. Direct evidence for the formation of acetic acid and lead-acetate in the encapsulant ethylene vinyl acetate after prolonged damp-heat exposure could be found and directly related to cell corrosion effects paralleled by power losses.

KEYWORDS

climate sensitivity, climate specific accelerated ageing tests, correlation of power and material degradation, database-advanced data treatment, nondestructive characterization

1 | INTRODUCTION

The PV market experienced drastic changes in the last decade, marked by a huge price drop for PV elements and the ongoing competition amongst different technological solutions and manufacturing locations. Nevertheless, the market shows enormous potential with high growth rates, not only but also in climatic regions with extreme environmental stress conditions such as high solar irradiation[1-4] at high altitudes or in arid areas.

Apart from initial failure modes which lead to a quick drop of the performance in the beginning of the working life of PV modules and are mostly caused by failures in manufacturing, transport, or installation ("infant-failures"),[5,6] performance losses of the modules due to continuous ageing and degradation of the materials/components ("midlife failures") are defining the long-term stability and profitability of PV systems.[3,7] Thus, artificial accelerated ageing tests, simulating this continuous degradation of PV modules under given stress conditions,[8-10] are a key procedure for an efficient and fast product improvement, especially for developing new PV modules/materials which are optimized for the use in specific climate regions. The big challenge in this respect is the adaption/advancement of existing standard procedures for PV modules/components testing like, eg, PV module design qualification and type approval (IEC 61215),[11] PV module safety requirements (IEC 61730),[12] or salt mist corrosion testing (IEC 61701)[13] in a way that reliable testing of PV modules (designed for certain climate conditions) is possible. This demanding task is addressed in several research activities, eg, within the PVQAT initiative,[14] the SERIIUS cooperation,[15] the investigation on PV system failures within the IEA PVPS Task 13,[16] the Australian PV Institute survey,[17] and the Austrian research project INFINITY.[18] In addition, activities are going in the standardization community to develop climate specific test procedures[19] and high operating temperature,[20] but up to now no final document is published.

In general, accelerated ageing tests with repeated application of combined climatic and environmental stresses (temperature, temperature cycles, humidity, irradiation, mechanical load, salt mist) aim to cause material degradation effects, performance losses, and failures comparable to those observable in real-life ageing under similar stresses.[8-10]

In the work presented, which is part of the Austrian research project INFINITY, the objective was to develop optimized, climate specific accelerated ageing test procedures for PV modules to be installed in different climate zones (arid, tropical, moderate, and alpine). Thus, a matrix of 14 ageing test procedures with sequential or constant stress application was designed. Numerous test modules with identical composition and design were produced and pre-characterized. Then, sets of three modules each were exposed to the various predefined stress tests, and the electrical performance of the modules as well as physical and chemical changes of the materials were monitored with nondestructive characterization methods during increasing ageing time (several intermediate stages). With the aim to provoke degradation processes in the test modules which resemble best the failure modes observed at naturally aged modules in the respective climate zones, the stress test conditions for the climate specific accelerated ageing tests are optimized.

Assembling these characterization data in a tailored database and combining it with the stress conditions and ageing times applied form the basis for advanced data treatment and allow for the development of a model for the simulation of degradation effects under predefined environmental and climatic conditions. This can provide the manufacturers a tool which allows for climate-specific testing of materials, individual components, and whole module assemblies in tailored, accelerated ageing test procedures (essential for efficient and fast product development).

2 | EXPERIMENTAL

2.1 | Test modules

Identical test modules with respect to composition (poly c-Si cells, ethylene vinyl acetate copolymer (EVA) encapsulation, polyester (PET)-based backsheet with flour-coating on the inner side) and module design (six cells, glass/backsheet) were used for the extensive accelerated ageing test program. At a time, at least three identical test modules were exposed to each test procedure to increase the statistic reliability of the test results. All available information of the test modules (groups of 3) were collected in a logbook.

All samples were characterized in detail (1) before and after light stabilization (40 kWh/m^2), (2) during (six intermediate stages), and (3) after the accelerated ageing procedure. Electrical characterization was done by power (current-voltage [I-V] and electroluminescence [EL] measurements), the encapsulation was nondestructively analysed by ultraviolet (UV)-fluorescence imaging and spectroscopy, and the polymeric backsheet by colour and Fourier transform infrared (FTIR) spectroscopic measurements.

2.2 | Developed accelerated ageing tests

Based on a definition of four specific climate profiles (humid and hot—tropical, dry and hot—arid, warm temperate—moderate and cold temperate/continental—alpine), a program has been worked out with 14 climate profile specific test procedures for accelerated ageing tests (see Table 1). Several test procedures with either (1) combined stress application under constant conditions (eg, moderate 1 and tropical 1) or (2) repeated sequential exposure to specific stresses (eg, moderate 2-5) were developed. A detailed description of the developed accelerated ageing tests is given in the results and discussion section (chapter 3) of this paper. The temperatures given in the descriptions of the ageing actions (Table 1) are all the pre-set chamber temperatures of the climate chambers. It has to be taken into account that in the case of additional irradiation stress (sunlight simulation 300-2500 nm with metal halide lamps), the module temperatures were 10°C-15°C higher than the chamber temperature.

The chosen allocation was corresponding to the classification by Köppen Geiger[21-23] for the main climate groups.

A tropical/megathermal climates
B dry (desert and semi-arid) climates
C temperate/mesothermal climates
D continental/microthermal climates
E polar climates

The relation of the developed 14 climate specific ageing test profiles to the five Köppen-Geiger main climate groups is given in Table 2.

2.3 | Characterization methods

A detailed analysis/characterization of all modules was performed (1) before, (2) during (six intermediate stages), and (3) after the accelerated ageing test.

2.3.1 | Electrical measurements

By means of IV-characteristics measurements, the open circuit voltage (U_{OC}), short circuit current (Isc), series resistance (R_S), shunt/parallel

TABLE 1 Developed matrix of INFINITY climate specific accelerated ageing test procedures (T = temperature, H = humidity, I = irradiation, DML = dynamic mechanical load, TC = thermal cycles)

	Duration		Temp.	Humidity	Irradiance	DML	Salt/Sand	TC	Intervalls
Reference	1000 h	1	85°C	85%	-	-	-	-	Constant
Moderate1	1000 h	1	85°C	85%	1000 W/m^2	-	-	-	Constant
Moderate2	1000 h = 7 cycles	1 2	60°C 85°C	40% 85%	1000 W/m^2 -	- -	- -	- -	48 h 96 h
Moderate3	1000 h = 7 cycles	1 2 3	60°C 85°C -	40% 85% -	1000 W/m^2 - -	- - 1000 c	- - -	- - -	48 h 96 h 24 h
Moderate4	1000 h = 7 cycles	1 2 3	60°C 85°C 60°C	40% 85% -	1000 W/m^2 - -	- - -	- - Salt-mist	- - -	48 h 96 h 24 h
Moderate5	3000 h = 7 cycles	1 2 3	60°C 85°C −40/+85°	40% 85% -	1000 W/m^2 - -	- - -	- - -	- - 50 c	48 h 96 h 300 h
Tropical1	3000 h	1	85°C	85%	-	-	-	-	Constant
Tropical2	3000 h	1	90°C	90%	-	-	-	-	Constant
Tropical3	1000 h = 7 cycles	1 2	80 °C 90°C	60% 90%	1000 W/m^2 -	- -	- -	- -	48 h 96 h
Arid1	1000 h	1	95°C	50%	1200 W/m^2	-	-	-	Constant
Arid2	1000 h = 7 cycles	1 2 3	80 °C 95°C -	40% 50% -	1200 W/m^2 - -	- - 1000 c	- - -	- - -	48 h 48 h 24 h
Arid3	1000 h = 7 cycles	1 2 3	80 °C 95°C 60°C	40% 50% -	1200 W/m^2 - -	- - -	- - Sand abrasion	- - -	48 h 48 h 48 h
Alpin1	1000 h	1	85°C	85%	1200 W/m^2	-	-	-	Constant
Alpin2	1000 h	1 2	85°C -	85% -	1200 W/m^2 -	- 1000 c	- -	- -	48 h 24 h
Alpin3	1000 h = 3 cycles	1 2	60°C 85°C -	40% 85% -	1200 W/m^2 - -	- - -	- - -	- - 50 c	48 h 96 h 300 h

TABLE 2 Relation of Köppen Geiger climate zones to INFINITY climate specific accelerated ageing tests (T = temperature, H = humidity, I = irradiation, DML = dynamic mechanical load, TC = thermal cycles)

	INFINITY	
Köppen-GeigerClimate Classification Scheme	**Code of ageing test**	**Applied stresses**
A (tropical)	Tropical1 Tropical2 Tropical3	T, H Elevated T, H Elevated T, H; I
B (arid)	Arid1 Arid2 Arid3	High T, I + DML + sand abrasion
C (temperate) Warm moderate	Moderate1 Moderate2 Moderate4	T, H, and I 1) I, 2) T, H 3) Saltmist
D (continental) Cold moderate	Moderate3 Moderate5 Alpin1 Alpin2	3) DML 3) TC T, H, high I + DML
E (polar)	Alpin3	1) high I; 2) T, H; 3) TC

resistance (R_P), maximum power point (P_{MPP}), voltage at MPP (U_{MPP}), current at MPP (I_{MPP}), and fill factor (FF) were determined. The IV measurements of all test modules before, at the intermediate stages, and after the accelerated ageing tests were in accordance with IEC 61215.[11,24] The electrical performance was measured under laboratory standard conditions (25°C; 1000 W/m^2 with air mass 1.5 spectral distribution) using a PASAN High^{LIGHT} Very Large Module Tester flash cell tester. The High-^{LIGHT} Very Large Module Tester is designed to flash a surface up to 3 by 3 m. In our case, the six-cell modules are measured before and after aging instances, so only the relative measurement uncertainty is relevant. The excellent accuracy of the flasher systems power measurement results in a relative uncertainty of less than 0.5%, within 95% confidence.

The IV measurements of the test modules were performed "fresh out of the box" and after light stabilization (LID) with 40 kWh/m^2. As all modules have an identical bill of material, including the same cell type (standard, non PERC), it was sufficient to use always the same light dose for LID stabilization, instead of following the exact Module Qualification Test (MQT) 19.1—initial stabilization with three consecutive power measurements,[11] because stabilization is reached after less than 10 kWh for this standard crystalline cell type. For the database and all further data treatments (modelling), the light stabilized values of the electrical performance were taken as starting values (ageing instance = 0); all relative values are referenced to these original states (100% values). The performance values obtained for the fresh out of the box-modules were attributed to an ageing instance value of −1 and were typically higher than the P_{MPP} values obtained after LID.[25-28]

2.3.2 | Electroluminescence measurements (EL)

Electroluminiscence measurements take advantage of the radiative interband recombination of excited charge carriers in solar cells. For EL investigations, the module is operated as a light emitting diode meaning that current is applied in reverse direction. The emitted radiation due to recombination effects can be detected with a sensitive Si-CCD-camera. The wavelength window of the Si-CCD camera is 300 to 1100 nm. The solar cells are supplied with a defined external excitation current (current applied $\leq$ Isc of the cell or module) while the camera takes an image of the emitted photons. Damaged areas of a solar module appear dark or radiate less than areas without defects. EL has proven to be a useful tool for investigating electrical inhomogeneities caused by intrinsic defects (eg, grain boundaries, dislocations, shunts, or other process failures) and extrinsic defects (eg, cell cracks, corrosion, or interrupted contacts)[29-33]

To determine the influences of defects (eg, shunts), the EL behaviour of the test modules was investigated with different current densities: 10% and 100% of I_{SC}. When applying a low current density (10% of I_{SC} of the module), the shunts conduct most of the current. When applying higher current densities (~I_{SC}) by applying a higher voltage at the module, the conductivity of the positive-negative (p-n)-junction increases according to the non-linear (voltage/current) diode characteristic, compared with the (nearly constant) shunt conductivity, and shunts were less influential on the EL intensity distribution. Thus, with low current densities, the material properties can be investigated, while with high current densities, the properties of the electrical contacts predominately define the results and can be investigated.[34]

2.3.3 | UV-fluorescence measurements

Fluorescence is a form of luminescence and stands for the physical effect of the emission of light by a material that has absorbed light or other electromagnetic radiation. The emitted light (eg, in the visible region) has a longer wavelength than the absorbed radiation (eg, UV light). A fluorophore is thus a fluorescent chemical compound that can re-emit light upon light excitation and mostly contains several combined aromatic groups or other plane or cyclic molecules with several π bonds. Typical fluorophores are degradation products of polymers and/or additives with chromophoric/fluorophoric groups. The fluorescence behaviour of materials can be extinguished by "photo bleaching" effects which lead to a decrease in fluorescence due to reaction processes with, for example, oxygen.[6,31,35,36]

UV-fluorescence imaging (UVFI)

UV-fluorescence measurements were performed in dark environment by illumination of the PV modules with UV light and detection of the fluorescing light in the visible region by a photographic camera system (Olympus OM-D, equipped with long pass filter to cut-off the UV irradiation). Excitation with UV light was performed with a self-made UV

lamp,[37] consisting of three power-tuneable LED-arrays with an emission maximum at 365 nm and a short pass filter to cut off all visible light emitted. Power supply is a modified DC/DC converter with a controllable and piecewise constant voltage/constant current characteristic, providing a maximum DC power of 300 W, sourced by a 12 cell lithium-polymer accumulator with a capacity of 5000 mAh.[38,39] This characterization method is nondestructive, non-invasive, easy to handle, and fast (an exposure time of 30 seconds is sufficient to achieve a well-contrasted UV-fluorescence image of a module) [6, 39 40].

UV-fluorescence spectroscopy (UVFSp)

The setup for the UV-F spectroscopic measurements comprises a UV-light source (LED 380 or 365 nm) for excitation, which is mounted on a probe holder and directs a UV-light beam (diameter 3 mm) through the front glass of the PV module into the encapsulant. The detection of the fluorescent light occurs via an optical fibre (probe for reflexion/fluorescence measurement; ocean optics QR600-7-SR 125 BX) which is also installed in the probe holder device and channels the light into a UV/VIS spectrometer type Ocean Optics MAYA 2000 Pro (200-1100 nm).[40]

2.3.4 | Colour measurements

In order to determine the ageing induced colour changes of the backsheets, additional CIELAB colour difference measurements on the backsheets environmental surface were performed. A portable spectral photometer (type Datacolor CHECK II PLUS) was used; the measurements were performed according to standard EN ISO 11664-4 making use of the CIE L*a*b colour scale.[41] For the assessment, the delta values (ΔE, ΔL, Δa, and Δb) between the original and aged samples were used. The total colour difference is usually expressed by ΔE which includes lightness(+)/darkness(−) (ΔL), redness(+)/greenness(−) (Δa), and yellowness(+)/blueness(−) (Δb).[42] Colour changes (ΔE) between 0 and 1 are negligible as not detectable for the human eye.

2.3.5 | FTIR spectroscopy

Potential material degradation of the polymeric backsheet at the environmental side was analysed by attenuated total reflection (ATR) FTIR spectroscopy. The interaction (absorption) of electromagnetic radiation in the mid IR region (2.5-25 μm wavelength) with matter results in the excitation of molecular vibrations. An infrared spectrum shows the wavelengths where specific absorption takes place and gives thus information on the structure of molecules (qualitative analysis). ATR is a special sampling technique[43] which uses a property of total internal reflection resulting in an evanescent wave. A beam of infrared light is passed through the ATR crystal in such a way that it reflects at least once off the internal surface in contact with the sample. This reflection forms the evanescent wave which propagates into the sample. This method is surface sensitive, as the penetration depth into the sample is typically between 0.5 and 2 μm.[43] For the measurements, a portable ATR-FTIR spectrometer system (A2 Technologies; EXOSCAN) is utilized. The system uses a diamond ATR crystal in single reflexion mode with a diameter of 2 mm. The depth of penetration for infrared energy at 1700 cm^{-1} with this setup is ~2 μm.[42] The measurement parameters were set as follows: 40 scans were taken for background and for the sample with a resolution of 4 cm^{-1}. Three measurements points were taken for each sample.

2.4 | Database

All measurement results are organized in an optimized database, which forms the information base for setting up models for climate sensitive ageing and degradation processes/mechanisms. The database is structured around the modules (module = device under test), see general scheme given in Figure 1. Modules are logically connected via their specific ageing module groups with strictly associated ageing actions and instances. As stated above, a set of three identical modules is stored together in each specific ageing action (= accelerated ageing test as described in detail in Table 1) in order to increase the statistical reliability. Those triples are logically grouped in the database with the corresponding acquired measurement results being canonicalized and stored in the database as well. For future applications (modelling), all measurement information is kept as complete as possible; aggregation is avoided.

In a first step, the information outcome (results) of the various measurement methods and the corresponding measurement parameters of the used equipment had to be collected and harmonized. This process was recorded and documented in a collaboration platform (Mahara,[44] an ePortfolio-management platform). Naming conventions for each class of information, modules (device under test), ageing procedures, and measuring methods were agreed upon within the consortium. Exemplarily, the outcome of this harmonization process for the

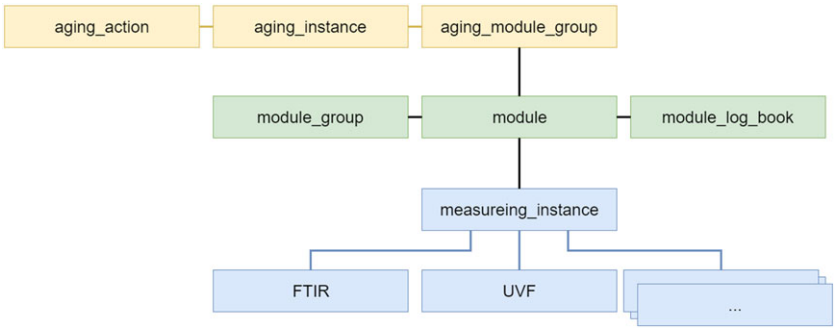

FIGURE 1 Database structure (simplified representation) [Colour figure can be viewed at wileyonlinelibrary.com]

IV-curve measurements is given in Figure 2, showing the nature of the (1) (raw) measured data, (2) computed to—information, (3) aggregated to—information and (iv) recorded data, which is finally stored first on the server and then built into the data base. A strict but explicit folder structure for collecting all measuring results was established at the server.

In the second step, all data of (1) the logbooks of the PV-test modules, (2) the ageing test procedures (ageing actions), and the (3) the characterization results were stored into a clearly defined folder structure on a server taking into account the file name conventions, data formats, and resolutions described in the Mahara platform.

In the third step, the database was generated from all stored data files. To build the database, SQLite[45] was used in conjunction with peewee (an object-relational mapper[46]). The database model classes, which are used by peewee to create and interact with the database, are provided to be used for the modelling phase. After configuring the path for the input measurement files and one for deploying the generated data base files, the program sets up the database automatically. Specific parsing scripts were developed for each type of measurement output files, thus, allowing for automated data base compilation without any error prone manipulation of the output files.

For the build of the database, first all the file names were parsed from the given input directory and checked against filename convention and folder structure. Then, the module-logbooks, which hold the overall life-cycle information of the tested module groups, were parsed, stored into data base, and logically linked to the respective test-modules. Then, "measurement_instances" were created for every ageing cycle applied to a distinct module, representing the whole set of measurement methods applied after the entire ageing cycle. Measurement information of each method applied was entered into

IV-curve (Current Voltage) aka flashertest

abbreviation	**IVSTC** (1000 W/m^2, 25°, AM 1.5 without spectral correction) **IVSTCS** (1000 W/m^2, 25°, AM 1.5 with spectral correction) **IVLIC** (low irrad cond, 200 W/m^2, 25°, AM 1.5)	
parameter	• Conditions (near STC, computed to STC) • cell area, DUT area • calc param (α, β, κ)	
measured data	• IV-curve (current, voltage) exceeding X and Y intercept • Irradiation • Temp DUT, $Temp_{CellRef}$	• G_{raw} [W/m^2] • V_{raw} [V] • I_{raw} [A] • Raw is valid ?
computed to	• IV-curve (current, voltage) @STC	• V_{comp} • I_{comp} • P_{comp} • computation is valid ?
aggregated to	• U_{oc} • I_{sc} • P_{mpp} • U_{mpp} • I_{mpp} • FF (fill factor) • cell efficiency • DUT efficiency • current density (J_{sc}) • R_s • R_p	• Voltage @open circuit [V] • Current @short cut [A] • Power @maximum power point [W] • Voltage @maximum power point [V] • Current @maximum power point [A] • P_{mpp} / (U_{oc} * I_{sc}) [%] • P_{mpp} / (NrOfCells * CellArea * $Irrad_{STC}$) [%] • P_{mpp} / (DUTArea * $Irrad_{STC}$) [%] • I_{sc} / cell area [mA/cm^2] • Δu/Δi slope at U_{oc} (-0.1 A:+0.1A) • Δu/Δi slope at I_{sc} (-0.1 V:+0.1V)

recorded data	• **$IV\text{-}curve_{raw}$, $IV\text{-}curve_{comp}$ @STC**
	• **U_{oc}**
	• **I_{sc}**
	• **P_{mpp}**
	• **FF (fill factor)**
	• **cell efficiency**
	• **DUT efficiency**
	• **current density (J_{sc})**
	• **R_s**
	• **R_p**
		• **IV-raw[firstValidcomp:lastValidcomp]**
		  ○ **V_{raw}[firstValidcomp:lastValidcomp]**
		  ○ **I_{raw}[firstValidcomp:lastValidcomp]**
		• **IV-curve[firstValidcomp:lastValidcomp]**
		  ○ **V_{comp}[firstValidcomp:lastValidcomp]**
		  ○ **I_{comp}[firstValidcomp:lastValidcomp]**

FIGURE 2 Filename convention, parameter, and description of the measured data for IV-curve measurement as specified in the Mahara platform [Colour figure can be viewed at wileyonlinelibrary.com]

specific tables; those entries refer to this specific "measurement_instance." This allows for simple, selective, and fast data base queries and avoids a full data base read. One resulting diagram of such a typical query (results of colour measurements of the backsheets of three test modules stored under moderate5 conditions) is shown in Figure 3.

The fully automated rebuild mechanism of the data base and persistent storage of all raw measurement information from all measurement devices and measurement instances allow for future adaptation of the data base and analysis algorithms. The script used for automated data base build is flexibly configurable to reflect changes in directories and committed value ranges.

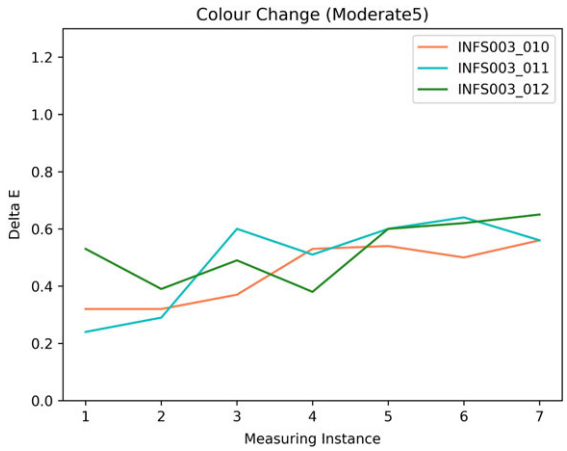

FIGURE 3 Colour change (ΔE) of three test modules which experienced ageing action moderate5; each measuring instance corresponds to 1 cycle as described in detail in Table 4 [Colour figure can be viewed at wileyonlinelibrary.com]

2.5 | Advanced data treatment

In order to identify which of the performed characterization methods describes best the impact of the applied accelerated ageing procedures, the changes over time were visualized. As mentioned above, a set of at least three identical modules was exposed to identical accelerated ageing procedures (repeatedly exposed to predefined stress conditions—as described in detail in Table 1). All modules under test were light-stabilized and pre-characterized before starting the accelerated ageing tests. These characterization results, obtained after this initial stabilization procedure, are considered as reference (starting point) for each individual module separately. This also marked the zero point on the ageing time scale. An ageing time scale was further defined by the time, the modules had been stored in the climate chambers, and thus, the ageing time (cumulated hours of storage time in the climate chamber) was calculated as multiples (cycle number, ageing instance) of storage time/cycle. It has to be noted that in this type of representation the accumulated hours of ageing correspond to ageing under different stress conditions as indicated for the different ageing actions (details are depicted in Table 1).

Under this assumption, the performance parameters for each module were plotted against the time of ageing. The FF and consequently the power at maximum power point (P_{MPP}) showed the most noticeable relative changes as shown exemplarily for the ageing actions moderate1-5 and tropical1 and 2 in Figure 4.

3 | RESULTS AND DISCUSSION

In the following, the results of the nondestructive characterization methods including electrical performance (I-V curves, EL images) and

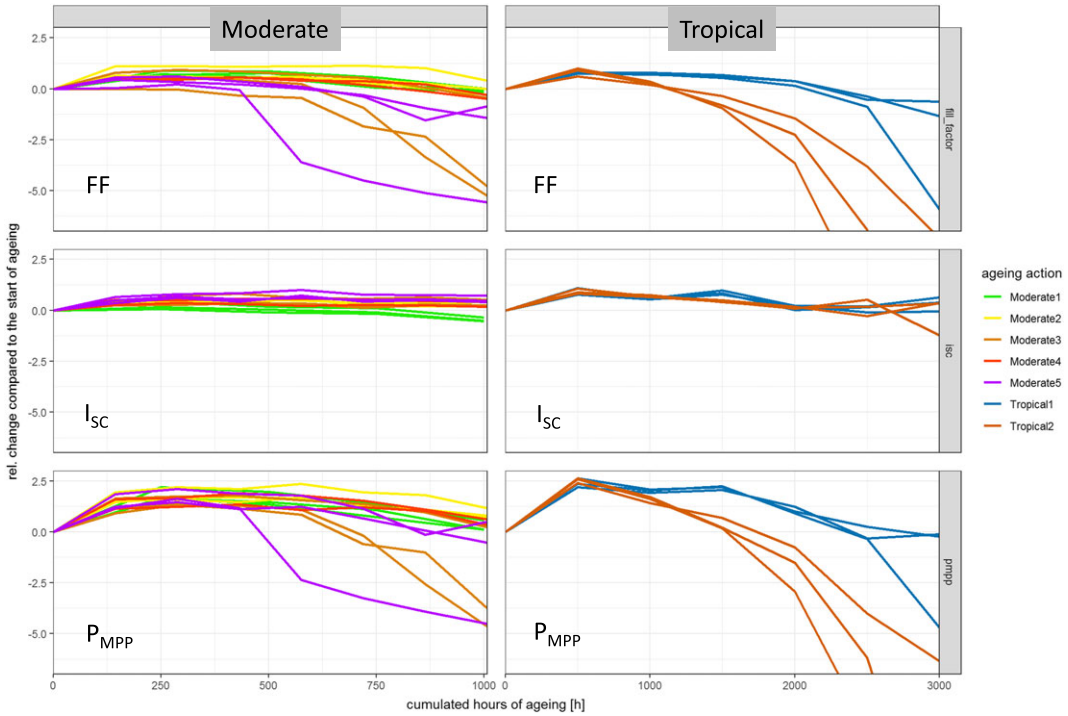

FIGURE 4 Relative change in FF (top), I_{SC} (middle), and P_{MPP} (bottom) for individual modules over ageing time, applying different colors for different accelerated ageing test procedures [Colour figure can be viewed at wileyonlinelibrary.com]

chemical and physical changes (FTIR and UV-fluorescence spectroscopic and imaging measurements as well as colour measurements) will be presented and discussed. They were applied in order to follow the module's ageing processes throughout the whole accelerated ageing procedure (original state, 6/3 intermediate stages, final state).

In specific cases, additional destructive material analysis (eg, spectroscopic and thermal analysis methods) were applied at the end of the accelerated ageing procedure in order to characterize in depth the degradation behaviour of the encapsulant after exposure to the corresponding stress conditions.

At the time the manuscript was prepared, ~2/3 of the accelerated ageing test procedures described in chapter 2.2 (and summarized in Table 1) were already finished, and all corresponding electrical and chemical characterization data incorporated in the database. In the following, the results of these ageing actions—namely reference, moderate1,2,3,4 and 5 as well as of ageing actions tropical1 and 2 will be presented and discussed.

3.1 | Ageing actions: MODERATE

As sort of reference accelerated ageing action, the 1000-h damp heat (DH; 85% relative humidity at 85°C constant for 1000 h) test according to standard IEC 61215, MQT 13[11] was chosen as it is the most frequently used test throughout the PV community.

As all PV modules experience apart from elevated temperature and humidity also irradiation stress, ageing action moderate1 was designed as an enhanced DH test with additional irradiation of 1000 W/m^2 (simulated sunlight, 300-2500 nm). Thus, direct comparison of the modules which experienced the reference test procedure and the moderate1 ageing action directly yield the influence of the additional irradiation stress (also resulting in a higher module temperature of +25°C). Table 3 summarizes the main results obtained with the nondestructive characterization methods. It can be clearly seen (Table 3, Figure 4) that compared with the light stabilized state, the performance of the test modules increased. This effect is especially strong for modules that experienced DH-storage[47-49] and attributed to increased transmittance of the encapsulation. After 1000-h ageing, hardly any changes were observed under reference and moderate1 conditions in the EL images and the colour of the backsheets (ΔE below 1, not detectable for the human eye).

The FTIR spectra of the outer surface of the backsheet of the modules exposed to ageing action moderate1 indicate that the additional irradiation initiated a beginning photo-degradation of the backsheets PET surface (changes in the relative intensities and shift in the absorption maxima of the bands typical for the ester group at 1714, 1244, 1119, and 1098 cm^{-1}).[42,50-52]

The most obvious difference induced by the enhanced stress conditions of moderate1 was observed in the UV fluorescence (see Figures 5 and 6). The presence of irradiation combined with the therefore induced higher module temperature gave significant rise to the formation of strong fluorescence in the encapsulant.[6,36,39,53] Furthermore, the formed fluorescence pattern is different for irradiated PV modules (UV-F observable in the whole front encapsulant) and DH-treated modules (weaker fluorescing effects in the areas between the cells). These effects are described in detail in Eder et al, Röder, and Hirschl et al.[39,54,55]

In contrast, the ageing actions moderate 2-5 (see Table 4) exhibit a repeated sequential application of various stresses. All these ageing actions start with an irradiation for 48 hours, followed by a DH phase for 96 hours. While moderate2 only comprises a repeated application of these two stress conditions; in moderate3, additional wind load is simulated by applying dynamic mechanical load cycles (1000 Pa, 1000 cycles). Moderate4 simulates additional salt stress (salt mist, 5% NaCl solutions), which PV modules might experience next to motorways in, eg, middle and northern Europe or northern America in wintertime or PV installation in coastal areas are exposed to. In ageing action moderate5, the test modules are additionally exposed to frequent temperature changes (50 temperature cycles, according to[11] MQT 11). Thermomechanical temperature cycle stress occurs (1) in areas with a big difference in day and night module temperature, eg, in arid regions under clear sky conditions and radiative cooling during the night, and (2) regions with frequent clouds and rapid changes between cloud enhancement and shaded low irradiance conditions.[47]

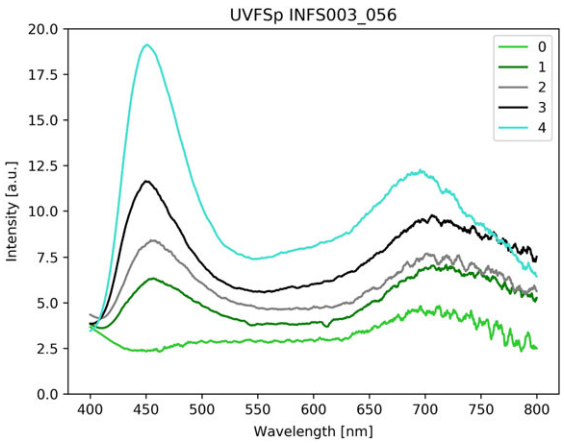

FIGURE 5 UV-fluorescence spectra of one test module (056) before, during, and after ageing action moderate1 (DH at 85°C/85% r.H. and irradiation at 1000 W/m^2); each measuring instance corresponds to 250-h exposure (plot resulting from database query) [Colour figure can be viewed at wileyonlinelibrary.com]

TABLE 3 Comparison of the main characterization results obtained for the test modules after 1000 h (i) reference/DH at 85°C/85% r.H. and (ii) moderate1/DH at 85°C/85% r.H. and irradiation 1000 W/m^2; values are averaged values obtained for three test modules

	ΔPMPP	EL/Si-Cells	Δ Colour/Backsheet	FTIR/Backsheet	UV-FSp/Encapsulation
Reference	+1.94%	No changes	+0.30	No changes	7.5@450 nm
Moderate1	+0.23%	No changes	+0.25	Beginning surface degradation of PET	19.1@450 nm

The P_{MPP} value after LID was taken as reference/starting point (=0).

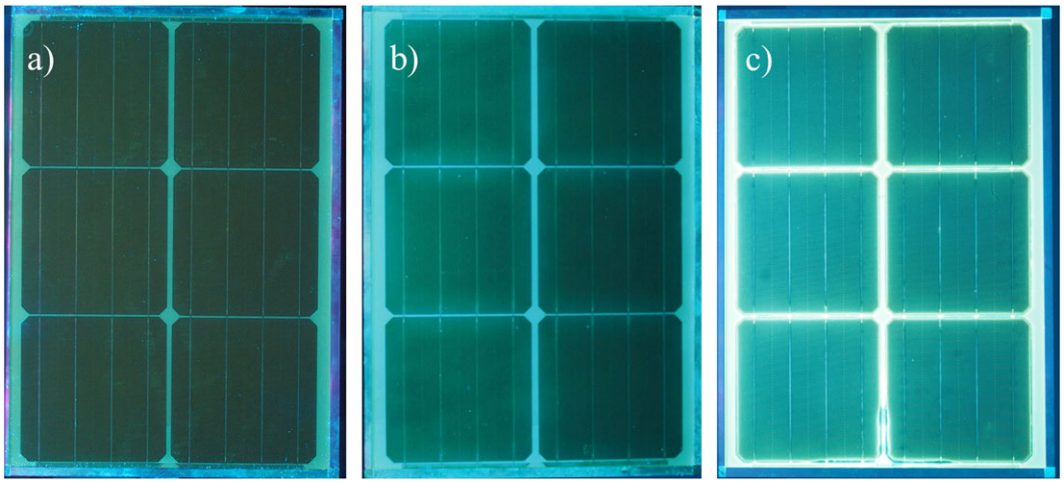

FIGURE 6 UV-fluorescence images of test modules (A) in the original state, (B) after 1000-h reference ageing (DH at 85°C/85% r.H.), and (C) 1000-h moderate1 (DH at 85°/85% r.H. and irradiation at 1000 W/m^2) [Colour figure can be viewed at wileyonlinelibrary.com]

TABLE 4 Detailed description of the ageing actions moderate 2-5

	Duration		T, °C	H, %	I, W/m^2	Extra	Intervals	Additonal Stress
Moderate2	1000 h = 7 cycles	1	60	40	1000	-	48 h	
		2	85	85	-	-	96 h	
Moderate3	1000 h = 7 cycles	1	60	40	1000	-	48 h	Wind load
		2	85	85	-	-	96 h	
		3	-	-	-	DML 1000c	24 h	
Moderate4	1000 h = 7 cycles	1	60	40	1000	-	48 h	Salt stress
		2	85	85	-	-	96 h	
		3	60	-	-	Salt mist	24 h	
Moderate5	3000 h = 7 cycles	1	60	40	1000	-	48 h	Frequent temperature changes
		2	85	85	-	-	96 h	
		3	−40/+85	-	-	TC 50c	300 h	

The changes in the electrical performance of the test modules, exposed to ageing actions moderate1-5 with increasing ageing time, are depicted in Figures 7 and 8. While exposure to irradiation and DH stress in constant (moderate1) or sequential order (moderate2) showed no remarkable change in the electrical performance after 1000 hours (seven cycles), additional DML (moderate3) and TC (moderate5) caused a decrease of 3.5% to 4% in P_{MPP} for individual test modules. Figure 9 shows EL images of a test module (012) of moderate5, which were recorded in parallel to the electrical performance measurements and clearly show a discrete event between cycle 3 and 4, indicating a connection problem for the black region at cell 6. This is in good agreement with the drop in P_{MPP} of this test module (012), depicted together with other I-V curve parameters in Figure 10. The drop in P_{MPP} goes along with a sudden rise in series resistance R_S, causing a drop of the FF, too. The DML treatment (moderate3, test module 006) induced cell cracks and microcracks which are paralleled with a decrease in the P_{MPP}.

It has to be noted that additional salt mist application (moderate4) had hardly any influence on the electrical or chemical degradation of the test modules (compared with moderate2).[56] This is not unexpected for polymeric materials, but multi material composites such as PV-modules containing several metallic interconnections might be prone to salt corrosion, in the case that insulations get cracked or delaminated. Furthermore, when the whole PV-system (including electrical wiring and mounting devices) is considered,[57] especially the metallic parts are sensitive to salt-corrosion effects.

The colour measurements gave only minor changes (Δ E between 0 and 1) for all modules exposed to moderate2,3,4, and 5. The FTIR measurements of the backsheets on the backside of the modules revealed (Figure 11) small but detectable changes in the maxima and broadness of the bands typical for the ester groups (1714, 1244, 1119, and 1098 cm^{-1}) indicating an onset of degradation reactions[42,50,51] and a change in the crystallinity of the PET.[58]

3.2 | Ageing actions: TROPICAL

Experience has shown that most PV materials and module types being presently in the market are tested with DH-test procedures, which are in accordance to standard IEC 61215 "Terrestrial photovoltaic (PV) modules—Design qualification and type approval",[11] but for much longer times than required[8,48,49] with the extended goal to make sure that the products are suitable also for tropical regions. Thus, when designing the accelerated ageing test procedures for the tropical climate, first prolonged ageing times at standard DH conditions (85°C/85% r.H.) were suggested (= tropical1). In the next step, temperature and humidity level were increased to 90°C/90% r.H. (= tropical2). In a third step (see Tables 1 and 2), the phases of

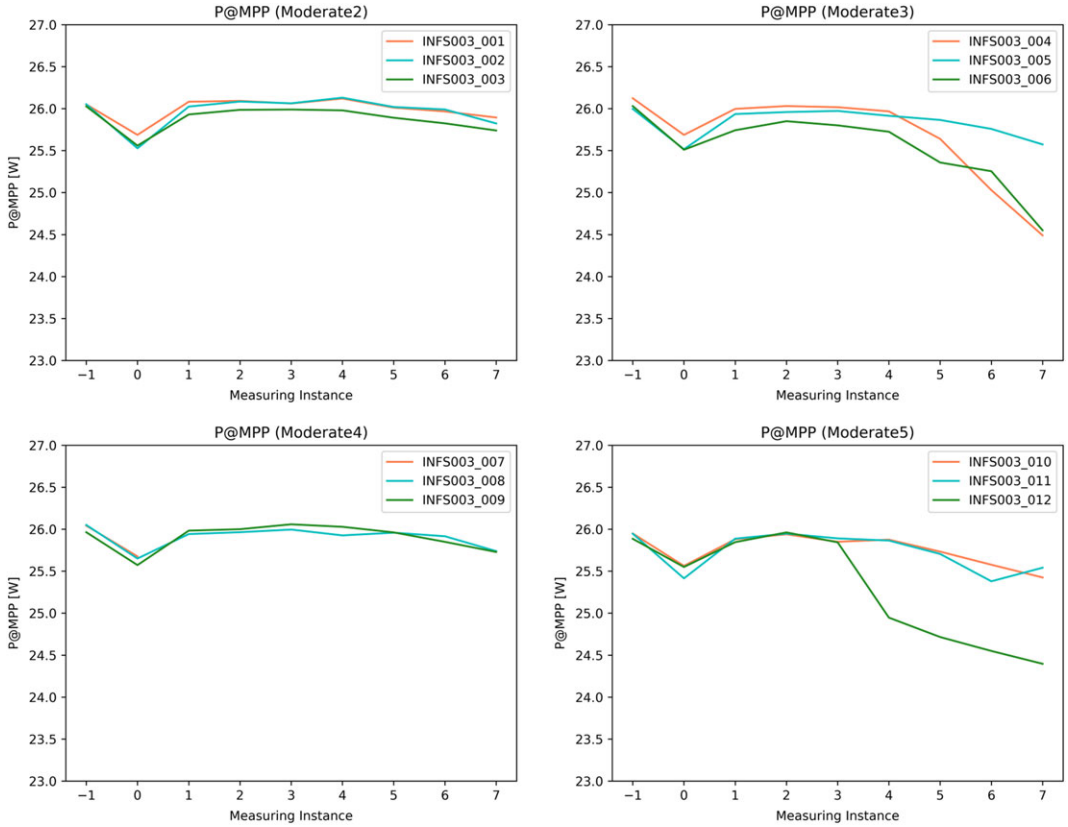

FIGURE 7 Electrical performance (given as P_{MPP}) of sets of three test modules each exposed to ageing actions moderate2-5 (resulting plots from database query). Measuring instance = 1 cycle as described in detail in Table 4 [Colour figure can be viewed at wileyonlinelibrary.com]

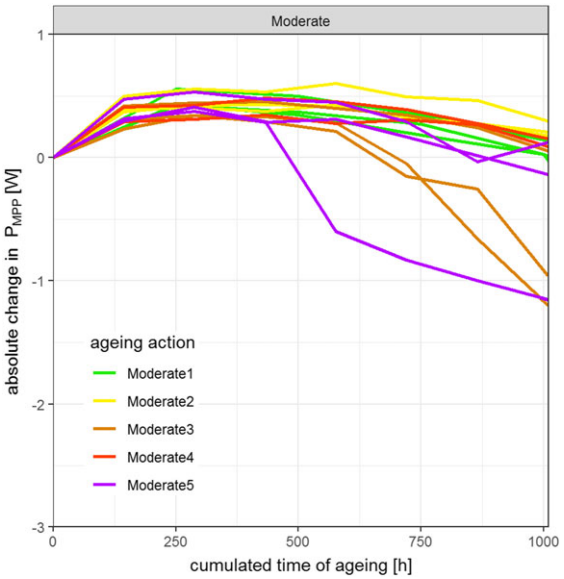

FIGURE 8 Electrical performance (given as absolute change in P_{MPP}) of sets of three test modules each exposed to either ageing action moderate1,2,3,4, or 5 with calculated cumulated ageing time [Colour figure can be viewed at wileyonlinelibrary.com]

constant DH-stress at increased temperature and humidity will be complemented with irradiation phases (= tropical3); the experiments for this ageing test, however, are still running.

In Figures 12 and 13, the development of the performance as a function of increasing storage time is shown for tropical1 and tropical2 in comparison to moderate1 (DH + irradiation). Especially, when plotting the change in power output against the cumulated time of ageing (Figure 13), it can be seen that the test modules showed stable performance under DH (85°C/85% r.H., tropical1) up to 1500 h. Then, with increasing exposure time, continuous power degradation is detected. When increasing chamber temperature and humidity (90°C/90% r.H., tropical2), the degradation starts already after 500 h of exposure. Also, the addition of irradiance to the DH conditions (moderate1) results in an onset of degradation at an earlier stage (after 250 h). Further characterization of these modules clearly shows that the loss of performance goes in line with cell corrosion processes, which are visible in the EL images recorded at 100% I_{SC} as dark areas of the cell, located along the connecting ribbons (Figure 14). The grade of propagation of dark cell areas at tropical2 (right column) corresponds to the progress at tropical1, but at half the time of exposure.

Additionally performed destructive material analysis by thermodesorption/gas chromatography and FTIR of the encapsulant EVA revealed the presence of acetic acid and acetates above these dark areas of the effected modules. Pb (IV)-acetate was detected in the interface of EVA to the soldered ribbons (Figure 15), and Na-acetate in the interface of EVA to the glass.

Furthermore, the FTIR spectra of the outer backsheet surface showed beginning degradation/hydrolysis of the PET after DH exposure, particularly after the enhanced conditions of tropical2. This is visualized by spectral changes occurring: (1) appearance of bands characteristic for vibrations of OH-groups (3465 cm^{-1}); (2) in the aliphatic

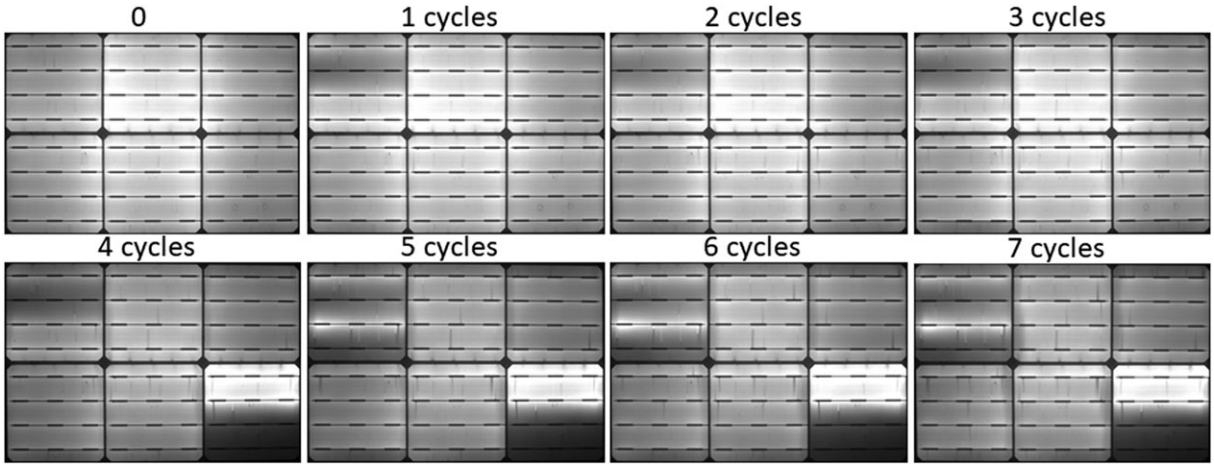

FIGURE 9 EL-images (8.2A = 100%Isc) of one test module (012) before, during, and after ageing action moderate5 (procedure for each test cycle: (A) irradiation at 1000 W/m^2, 60°C; (B) damp heat at 85°C/85% r.H.; (C) 50 temperature cycles −40 → +85°C)

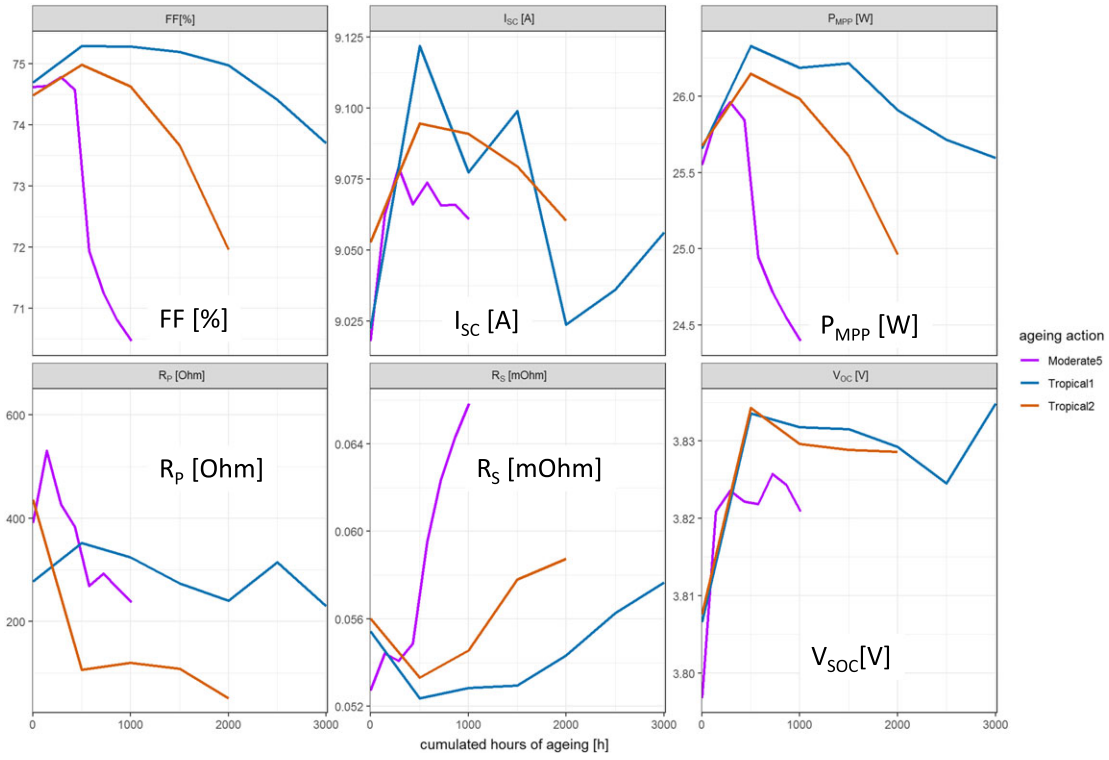

FIGURE 10 Values of P_{MPP}, I_{SC}, FF, V_{OC}, and series and parallel resistance R_S, R_P, derived from the I-V curve measurement at STC for the three modules 012, 021, and 030, before, during, and after ageing actions moderate5, tropical1, and 2, respectively. For ageing details, see Table 1 [Colour figure can be viewed at wileyonlinelibrary.com]

CH-absorption bands (3000-2800 cm^{-1} and 1470-1300 cm^{-1}); (3) broadening of the bands characteristic of the ester group (1715, 1240, and 1119-1098 cm^{-1}) as well as (3) spectral alterations of the bands typical for amorphous/crystalline PET regions.[50-52] Beginning material degradation is also measurable by the colour measurements (see Figure 16) which show elevated colour change values ΔE for the test modules exposed in ageing action tropical2. It has to be emphasized, however, that the outer layer of the PET backsheet comprises hydrolysis stabilized PET-grade and, thus, does not show strong degradation effects.[59] The core layer is more susceptible to hydrolytic degradation resulting in embrittlement and formation of cracks[9,42,52] with increasing DH exposure, especially at the conditions of tropical2 (90°C/90% r.H.).

The influence of the temperature and humidity stresses on the encapsulation material could be visualized nondestructively via UV-fluorescence measurements. The UV-F images of the test modules exposed to ageing action tropical1 and tropical2 show fluorescence patterns quite different from those PV-modules which experienced

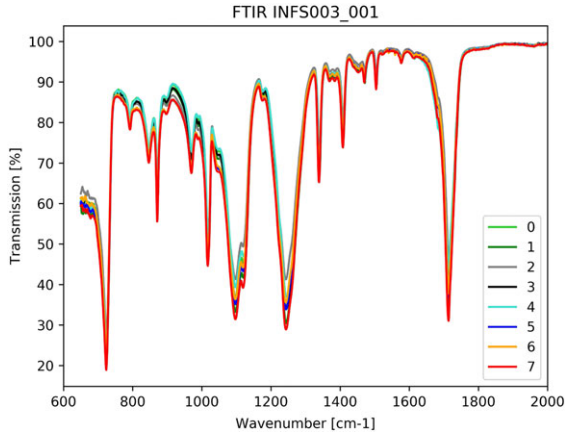

FIGURE 11 FTIR spectra of one test module (001) before, during, and after ageing action moderate2 (sequential exposure to irradiation at 1000 W/m^2 and DH at 85°C/85% r.H.); each measuring instance corresponds to 1 cycle as described in detail in Table 4 (plot resulting from database query) [Colour figure can be viewed at wileyonlinelibrary.com]

outdoor exposure or irradiation with artificial sunlight in accelerated ageing tests.[6,39,53-55] In real-life ageing, fluorescence is mainly trigged by elevated temperature and irradiation. Fluorescence building up in the polymer of the encapsulant upon DH storage is provoked by water vapour permeating via the polymeric backsheet into the encapsulant of the PV module. The evolution of the UV-fluorescence effects with increasing ageing time for tropical1 in shown in Figure 17.

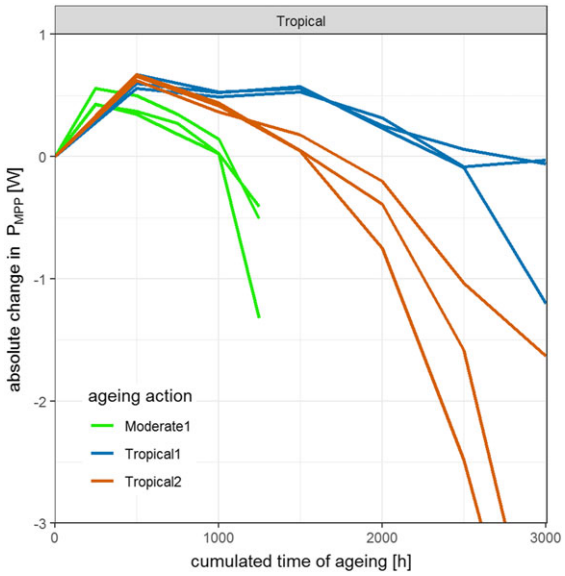

FIGURE 13 Electrical performance (given as absolute change in PMPP) of sets of three test modules, each exposed to either ageing action moderate1, tropical1, or tropical2 with calculated cumulated ageing time [Colour figure can be viewed at wileyonlinelibrary.com]

4 | SUMMARY AND OUTLOOK

As the PV market shows enormous potential with huge growth rates, not only but mainly in climatic-sensible regions, specific artificial ageing test procedures are a key point for an efficient and fast product

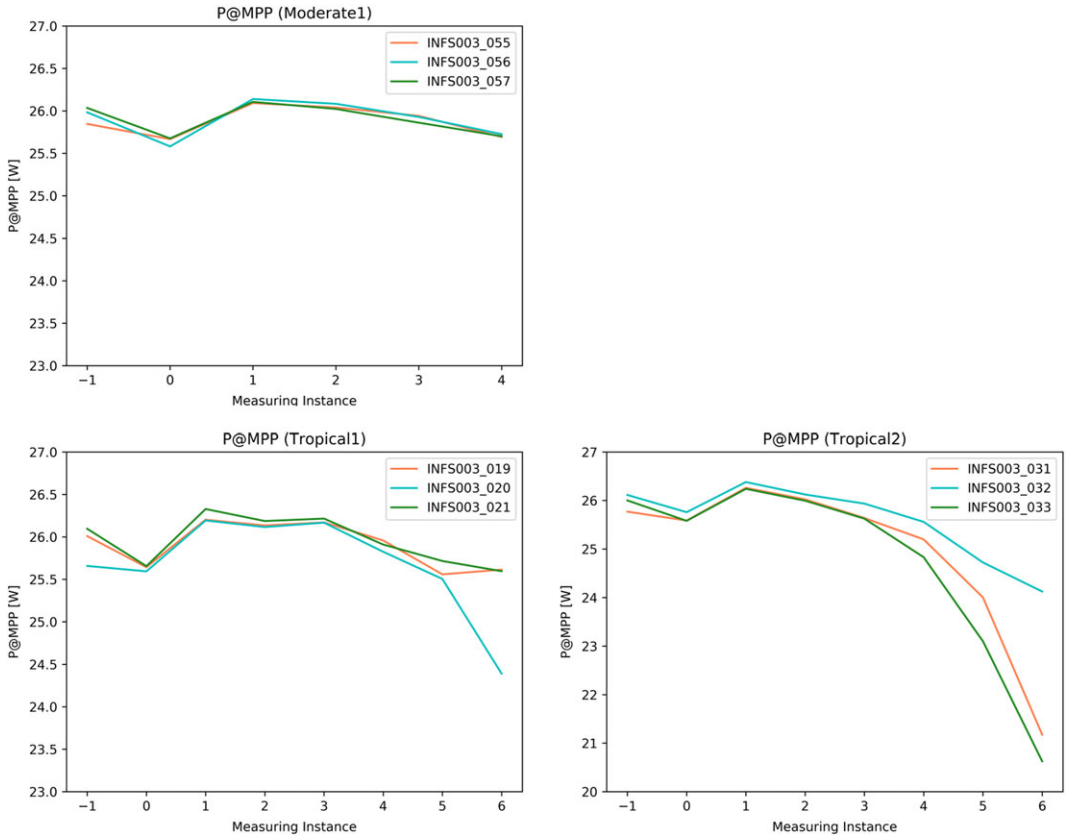

FIGURE 12 Electrical performance (given as P_{MPP}) of sets of three test modules, each exposed to ageing actions moderate1, tropical1, and tropical2 (resulting plots from database query). Measuring instance = 250 h for moderate1 and 500 h for the others [Colour figure can be viewed at wileyonlinelibrary.com]

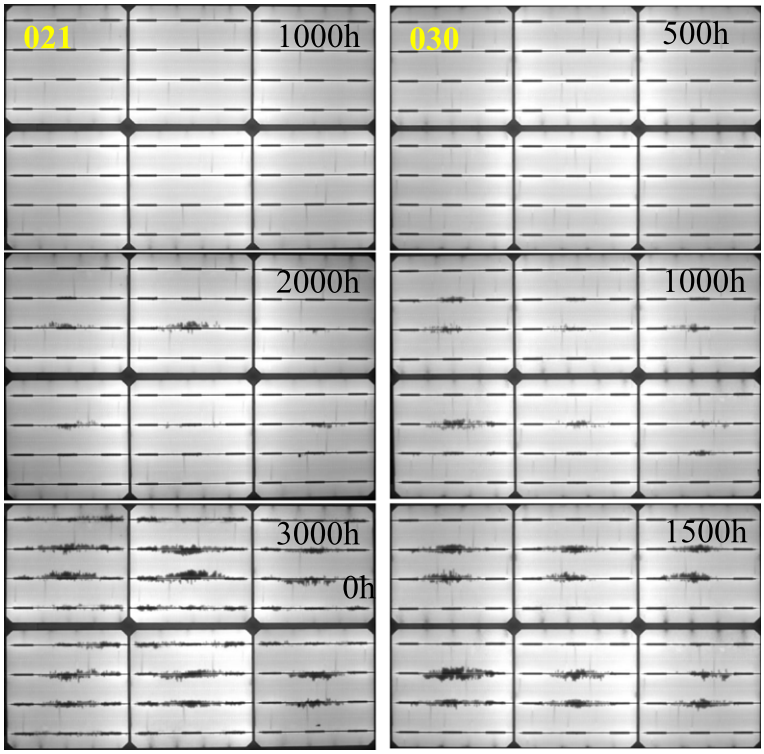

FIGURE 14 EL images (100%I_{SC}) left: of test module 021 (tropical1) after 1000, 2000, and 3000-h exposure; right: of test module 030 (tropical2) after 500, 1000, and 1500-h exposure. For detailed I-V curve parameters, see Figure 10 for comparison [Colour figure can be viewed at wileyonlinelibrary.com]

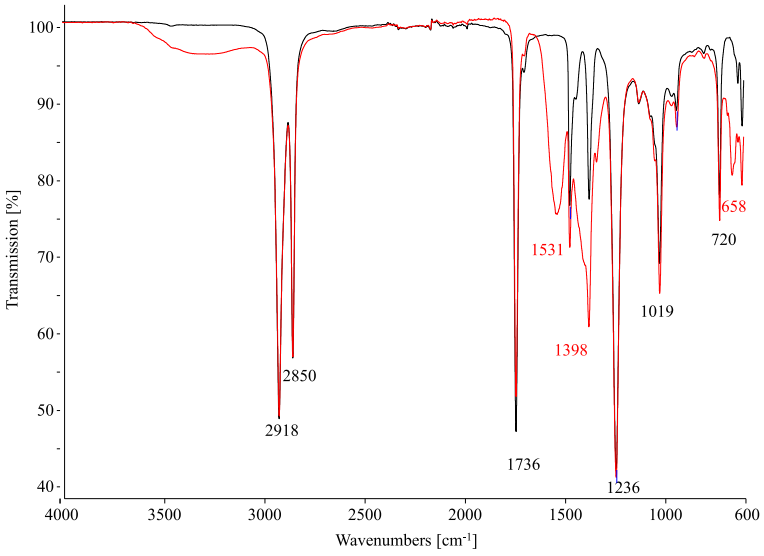

FIGURE 15 FTIR spectra of the EVA in the interface to the connector ribbons in the dark areas of the EL images of module 021 after 3000-h tropical1; black: spectrum of EVA intact, red: of EVA above the soldered ribbons, absorption bands typically for Pb (IV)-acetate are marked in red [Colour figure can be viewed at wileyonlinelibrary.com]

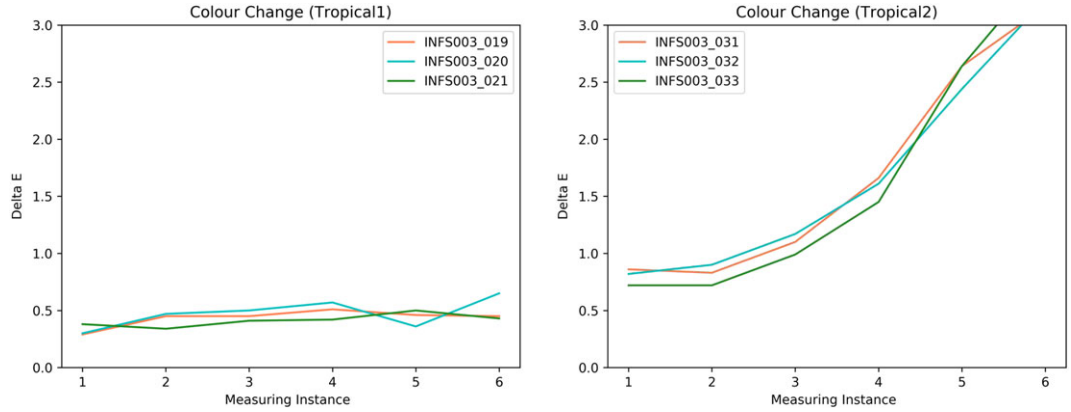

FIGURE 16 Colour change (ΔE) of three test modules which experienced left: ageing action tropical1, right: ageing action: tropical2; measuring instance = 500-h exposure as described in detail in Table 4 [Colour figure can be viewed at wileyonlinelibrary.com]

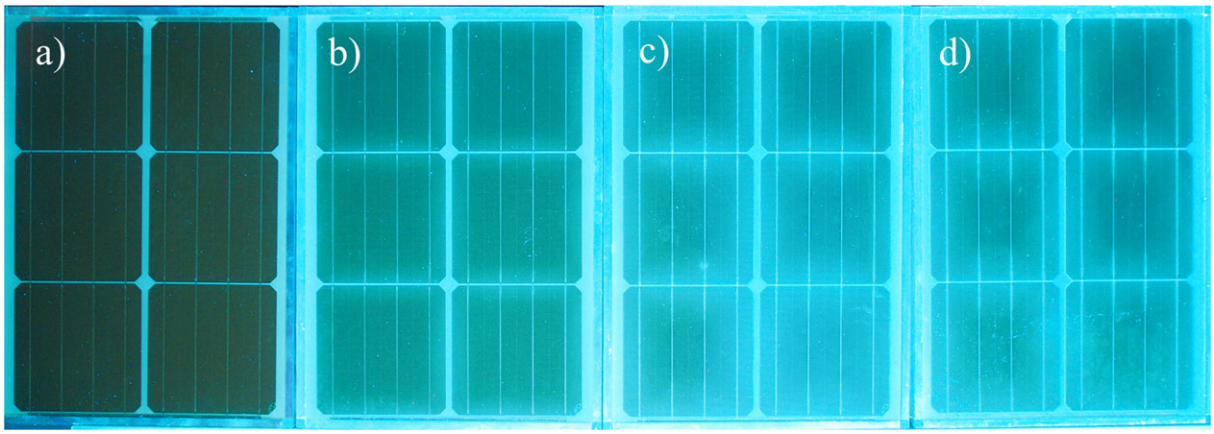

FIGURE 17 UV-fluorescence images of test modules (A) in the original state, (B) after 1000 h, (C) 2000 h, and (D) 3000 h of exposure to DH at 85°C/85% r.H. = ageing action tropical1 [Colour figure can be viewed at wileyonlinelibrary.com]

development of new PV modules/materials optimized for the use in specific climatic regions. Based on the definition of four climate profiles (dry and hot—arid, moderate, humid, and hot—tropical and high irradiation—alpine), a program was worked out with 14 climate specific test conditions for accelerated aging tests. The big challenge in this respect was the adaption/advancement of existing standard procedures for PV modules/components testing in a way that reliable testing for certain climatic conditions optimized PV modules is possible. The time-dependent repeated application of combined climatic and environmental stresses (temperature, temperature cycles, humidity, irradiation, mechanical load, salt mist) was used to induce performance losses, material degradation, and failures in test modules which resemble those effects occurring in real-life PV installations under comparable climatic and environmental conditions. For this demanding task, a large number of identical test modules with respect to composition (poly c-Si cells, EVA-encapsulation, PET-based backsheet) and module design (six cells, glass/backsheet) was manufactured. At a time, three test modules were exposed to each test procedure to get statistically more reliable results. A detailed nondestructive analysis/characterization of all modules was performed: (1) before; (2) during (six intermediate stages); and (3) after the accelerated ageing test. The nondestructive characterization methods used to follow the module's ageing processes throughout the whole accelerated ageing procedure were I-V characteristics measurements and EL images for the electrical performance evaluation and UV-fluorescence (spectroscopic and imaging) measurements, FTIR as well as colour measurements of the backsheets outer layer for recording of chemical changes of the encapsulant and backsheet.

At the time the manuscript was prepared, half of the accelerated ageing tests of the elaborated program (ageing actions reference, moderate1,2,3,4 and 5 as well as tropical1 and 2) were already finished, and all corresponding electrical and material characterization data incorporated in an optimized database. The database is structured around the test modules table with the PV modules logically connected via their specific ageing groups with strictly associated ageing procedures. As stated above, a set of three identical modules was exposed together in the respective climate specific ageing tests and subsequently characterized in order to increase statistical reliability of the measuring results. Those triples were logically grouped in the database as well. As this elaborate acquisition of data is aimed to be used for advanced data treatment and modelling applications in the near future, measurement information was kept as complete as possible, and aggregation was avoided.

The analysis of the data (queries from the database) and first approaches of advanced data treatment have already clearly shown that the electrical and material degradation of the test modules is dependent on (1) the type and combination, (2) duration, and (3) mode (sequential versus constant) of the stresses applied. On one hand, the simulation of environmental stresses like heavy snow and wind load and enhanced frequency of temperature cycling resulting in cell cracks and cell connector breakage could be demonstrated. Additional treatment in salty atmosphere, on the other hand, did not show an accelerating effect on degradation on the electrical or material (polymers, glass) side. The accelerating effect of enhanced temperature, humidity, or additional irradiation on the degradation of power and materials could be shown very well. Direct evidence for the formation of acetic acid and lead-acetate in the encapsulant EVA after prolonged damp-heat exposure could be found and directly related to cell corrosion effects paralleled by power losses.

4.1 | OUTLOOK

- finalize the climate specific accelerated ageing tests and data accumulation in the data base and use assembled results and information as a basis for a model allowing for simulation of degradation effects under predefined environmental and climatic conditions
- provide the manufacturers a tool which allows for climate-specific testing of materials, individual components, and whole module assemblies in tailored, accelerated ageing test procedures (essential for efficient and fast product development)
- continue and enhance the destructive material analysis (eg, mechanical, physical, and thermal analysis) at the end of the accelerated ageing tests in order (1) to characterize the ageing and degradation behaviour of the PV materials after exposure to the different stress conditions and (2) derive the prevailing degradation modes for the different climate profiles.

- optimize the climate specific artificial test procedures in respect to the highest possible accordance of the therein induced failures with the failures occurring in real-life aged PV-modules.

ACKNOWLEDGEMENTS

This work was funded by the Austrian Climate and Energy Fund and the Austrian Research Promotion Agency (FFG) in the framework of the Austrian "Energy Research Program" under project 850414 "INFINITY."

ORCID

Gabriele C. Eder http://orcid.org/0000-0003-0397-8453

REFERENCES

1. *Renewable Capacity Statistics 2018*. Abu Dhabi: International Renewable Energy Agency (IRENA); March 2018 ISBN: 978-92-9260-057-0.
2. Report IEA PVPS T1-32:2017: trends 2017 in photovoltaic applications, http://www.cansia.ca/uploads/7/2/5/1/72513707/iea_pvps_annual_report_2017__140518.pdf
3. Jordan DC, Kurtz SR, VanSant K, Newmiller J. Compendium of photovoltaic degradation rates. *Prog Photovolt Res Appl*. 2016;24(7):978-989. https://doi.org/10.1002/pip.2744.
4. Ferrada P, Rabanal Arabach J, Cabrera E, et al. AtaMo: PV meets the high potential of the Atacama Desert. *PV Tech Power*. 2015;5:55.
5. Wohlgemuth J, Cunningham D, Nguyen A, Kelly G, Amin, D. "Failure modes of crystalline Si modules", PV Module Reliability Workshop 2010.
6. Report IEA-PVPS T13–01:2014: Köntges M, Kurtz S, Packard C, Jahn U, Berger KA, Kato K, Friesen T, Liu H, Van Iseghem M, Wohlgemuth J, Miller D, Kempe M, Hacke P, Reil F, Bogdanski N, Herrmann W, Buerhop-Lutz C, Razongles G, and Friesen G: Review of failures of photovoltaic modules. IEA 2014, 114 p.; see http://www.iea-pvps.org/index.php?id=275
7. Wohlgemuth J. Standards for PV modules and components—recent developments and challenges. 27th European PVSEC 2012, Frankfurt, Germany.
8. Peike C, Hoffmann S, Dürr I, Weiß KA, Bogdanski N, Köhl M. PV module degradation in the field and in the lab—how does it fit together? 29th European PVSEC 2014, Amsterdam, The Netherlands.
9. Gambogi W, Kopchick J, Felder T, et al. Sequential and weathering module testing and comparison to fielded modules. NREL PV Module Reliability Workshop 2015.
10. Koehl M. Possibilities of accelerated life testing for different climates. Presentation at the IEC TC82 (Photovoltaic) WG2 (Modules) meeting at Estes Park, Colorado, USA, 49 p., Oct. 2016.
11. International Standard IEC 61215 Series. *Terrestrial Photovoltaic (PV) Modules—Design Qualification and Type Approval—Part 1: Test Requirements, and—Part 2: Test Procedures*. Edition 1.0 ed. ; 2016.
12. International Standard IEC 61730 Series. *Photovoltaic (PV) Module Safety Qualification—Part 1: Requirements for Construction; Part 2: Requirements for Testing*. Edition 2.0 ed. ; 2016.
13. International Standard IEC 61701. *Salt Mist Corrosion Testing of Photovoltaic (PV) Modules*. Ed 20 ed. :2011.
14. International PV Quality Assurance Task Force (PVQAT), http://www.pvqat.org/project-status/module-durability.html
15. Solar Energy Research Institute for India and the United States (SERIIUS), http://www.seriius.org/
16. International Energy Agency, Photovoltaic power systems programme, IEA PVPS Task 13 Performance and Reliability of Photovoltaic Systems. Data collection Documents available at http://iea-pvps.org/index.php?id=344
17. Zaman A, Parlevliet D, Calais M, et al. In: Watt M, Passey R, eds. *PV System Reliability—Preliminary Findings from the PV Module and System Fault Reporting Website*; 2015 Proc. APVI 2014, Sydney, http://apvi.org.au/solar-research-conference/proceedings-apsrc-2014/, PV Module and System Fault Reporting Portal https://www.surveymonkey.com/r/pvwebportal?sm=JFgKazY64MmBBZeTd4MZl7GNSzQdYODkYATq3zc%2fNG8%3d
18. Austrian Research project Infinity, 2015-2018, "Climate sensitive Photovoltaics".
19. International Standard IEC 62892 Test procedure for extended thermal cycling of PV modules, Ed.1.0: Actual draft: 82/1344/CDV, 2018.
20. International Standard IEC TS 63126 ED1 guidelines for qualifying PV modules, components and materials for operation at higher temperatures. Actual Draft 82/1216/NP.
21. Geiger R. *Classification of Climates after W. Köppen, Landolt-Börnstein—Zahlenwerte und Funktionen aus Physik, Chemie, Astronomie, Geophysik und Technik*. alte Serie. 3 Berlin: Springer; 1954:603-607.
22. Rubel F, Brugger K, Haslinger K, Auer I. The climate of the European Alps: shift of very high resolution Köppen-Geiger climate zones 1800-2100. *Meteorol Z*. 2017;26(2):115-125.
23. Updated Köppen-Geiger climate classification web site. Provides global data, world maps and computer animations, published by Kottek et al. (2006), Rubel and Kottek (2010) and Rubel et al. (2017). http://koeppen-geiger.vu-wien.ac.at/
24. International Standards IEC 60904–9:2007. *Photovoltaic Devices—Part 9: Solar Simulator Performance Requirements*. Edition 2.0 ed. ; 2007.
25. Fischer H, Pschunder W. Investigation of photon and thermal induced changes in Silicon solar Cells 10th IEEE Photovoltaic Specialists Conf., 1973, 404–411 p.
26. Schmidt J, Aberle AG, Hezel R. Investigation of carrier lifetime instabilities in Cz-grown silicon. 26th PVSC, Anaheim, CA, Sept 30 - Oct 3, 1997.
27. Sopori B, Basnyat P, Shet S, Mehta V, Binns J, Appel J. Understanding light-induced degradation of c-Si solar cells. 38th IEEE photovoltaic specialists conference, Austin, Texas June 3–8, 2012.
28. Ebner R, Újvári G, Mühleisen W, Hirschl Ch, Eder GC, Voronko Y, Vollmaier F. Importance of power stabilization of crystalline PV modules. EU 33rd PVSEC, 2018.
29. Wang G, Gong H, Zhu J. Failure analysis of dark cell detected by electroluminescence (EL). 28th European PVSEC 2014, 4AV.5.1, 3173–3179 p.; https://doi.org/10.4229/28thEUPVSEC2013-4AV.5.1
30. Köntges M, Siebert M, Hinken D, Eitner U, Bothe K, Potthof T. Quantitative analysis of PV-modules by electroluminescence images for quality control. 24th European PVSEC 2009, 4CO.2.3, 3226–3231 p.; https://doi.org/10.4229/24thEUPVSEC2009-4CO.2.3
31. Report IEA-PVPS T13–09:2017: Köntges M, Oreski G, Jahn U, Herz M, Hacke P, Weiss KA, Razongles G, Paggi M, Parlevliet D, Tanahashi T, French HR, Richter M, Tjengdrawira C, Morlier A, Li H, Perret-Aebi LE, Berger KA, Makrides G, Herrmann W: Assessment of photovoltaic module failures in the field. IEA 2017, 123 p. see http://www.iea-pvps.org/index.php?id=435
32. Report IEA-PVPS T13–10:2018: Jahn U, Herz M, Köntges M, Parlevliet D, Paggi M, Stein JS, Tsanakas I, Berger KA, Ranta S, French RH, Richter M, Tanahashi T, Friesen G, Hottenrott D. Review on infrared and electroluminescence imaging for PV field applications, 2018. http://iea-pvps.org/index.php?id=480
33. Ebner R, Zamini S, Újvári G: Defect analysis of different photovoltaic modules using electroluminescene (EL) and infrared (IR)-thermography. 25th European PVSEC 2010, 1DV.2.8., https://doi.org/10.4229/25thEUPVSEC2010-1DV.2.8
34. Crozier JL: Identifying voltage dependent features in photovoltaic modules using electroluminescence imaging. 29th EU-PVSEC, 2014.

35. Pern FJ. Factors that affect the EVA encapsulant discoloration rate upon accelerated exposure. *Sol Energy Mater Sol Cells*. 1996;41-41:587-615. https://doi.org/10.1016/0927-0248(95)00128-X

36. Pern FJ, Glick SH. Fluorescence analysis as a diagnostic tool for polymer encapsulation processing and degradation. AIP Conference Proceedings 306, 573, 1994; https://doi.org/10.1063/1.45730.

37. Knöbl K, Experimental UV lamp assembly, University of Applied Sciences Technikum Vienna, 2016.

38. Mühleisen W, Eder GC, Voronko Y, et al. Outdoor detection and visualization of hailstorm damages of photovoltaic plants. *Renew Energy*. 2018;118:138-145. https://doi.org/10.1016/j.renene.2017.11.010

39. Eder GC, Voronko Y, Hirschl C, Ebner R, Újvári G, Mühleisen W. Non-destructive failure detection and visualization of artificially and naturally aged PV modules. *Energies*. 2018;11(5):1053. https://doi.org/10.3390/en11051053

40. UVfSp Setup.

41. International Standard ISO 11664-4: (CIE S 014-4/E:2007). *Colorimetry —Part 4: CIE 1976 L*a*b* colour space*. Ed 1.0 ed. ; 2008.

42. Voronko Y, Eder GC, Knausz M, Oreski G, Koch T, Berger KA. Correlation of the loss in photovoltaic module performance with the ageing behaviour of the backsheets used. *Prog Photovolt Res Appl*. 2015;23(11):1501-1515. https://doi.org/10.1002/pip.2580.

43. Mirabella FM Jr. Practical Spectroscopy Series. In: *Internal Reflection Spectroscopy: Theory and Applications*. Marcel Dekker, Inc.; Marcel Dekker, Inc.; 1993:17-52.

44. Mahara. The open sources e-portfolio management platform; https://mahara.org

45. Relational Data Base Engine SQLite, https://sqlite.org

46. Object-Relational Mapping tool (ORM) Peewee, peewee-orm.com.

47. Bosco NS, Silverman T, Kurtz S. Climate specific thermomechanical fatigue of photovoltaic module solder bonds. *Microelectron Reliab*. 2016;62:124-129. https://doi.org/10.1016/j.microrel.2016.03.024.

48. Osterwald CR, McMahon TJ. History of accelerated and qualification testing of terrestrial photovoltaic modules: a literature review. *Prog Photovolt Res Appl*. 2009;17(1):11-33. https://doi.org/10.1002/pip.861

49. Jahn U. PV module reliability issues including testing and certification. IEA PVPS Task 13 Parallel Event at the 27th EU-PVSEC Frankfurt, 24.9.2012, www.iea-pvps.org/index.php?id=223&eID=dam_frontend_push&docID=1271

50. Zhu J, Koehl M, Hoffmann S, et al. Changes of solar cell parameters during damp-heat exposure. *Prog Photovolt*. 2016;24(10):1346-1358. https://doi.org/10.1002/pip.2793

51. Voronko Y, Eder GC, Knausz M, Oreski G, Koch T, Berger KA. Influence of environmental factors on the ageing behaviour of photovoltaic backsheets. Proc. European Weathering Symposium Bratislava 09.2013; CEEES Publication No 16, 2013; Editor: Dr.-Ing. Thomas Reichert; Publisher: GUS; ISBN 978-3-9813136-8-0.

52. Knausz M, Oreski G, Eder GC, et al. Degradation of photovoltaic backsheets: comparison of the aging induced changes on module and component level. *J Appl Polym Sci*. 2015;132(24). https://doi.org/10.1002/app.42093.

53. Schlothauer J, Jungwirth S, Röder B, Köhl M. Fluorescence imaging: a powerful tool for the investigation of polymer degradation in PV modules. Photovoltaics International 2010;10:149–154.

54. Röder B. The influence of different ageing factors on polymer degradation in photovoltaic modules investigated by luminescence detection. Proc. SPIE-Conf 7773.2010.

55. Hirschl Ch, Eder GC, Neumaier L, et al. Long term development of photovoltaic module failures during accelerated ageing tests. 33rd European PV-SEC 2017; 5BV.4.72, 1709–1712 p.; https://doi.org/10.4229/EUPVSEC20172017-5BV.4.72

56. Mathiak G, Althaus J, Menzler S, Lichtschläger L, Herrmann W. PV module corrosion from ammonia and salt mist—experimental study with full-size modules. 27th EU PVSEC 2012, 3536–3540 p.; https://doi.org/10.4229/27thEUPVSEC2012-4BV.3.44

57. Althaus J, Strohkendl K, Menzler S, Mathiak G. PV mounting system corrosion by salt mist—experimental study with full size mounting systems. 28th EU PVSEC, 2013, 2893–2896 p.; https://doi.org/10.4229/28thEUPVSEC2013-4CO.12.1

58. Miyake A. The infrared spectrum of polyethylene terephthalate. The effect of crystallization. *Aust J Polit Sci*. 1959;38:479-495.

59. Cheng-Tzu L, Chih-Hung W, Mu-Shih L. Poly (phenyl acrylate) and poly(p-methylphenyl acrylate) as photostabilizers, II. Protection of PET against photo-oxidation. *Polym Degrad Stab*. 2004;83:435-440.

How to cite this article: Eder GC, Voronko Y, Dimitriadis S, et al. Climate specific accelerated ageing tests and evaluation of ageing induced electrical, physical, and chemical changes. *Prog Photovolt Res Appl*. 2018;1–16. https://doi.org/10.1002/pip.3090